

## Increasing the yield in the exfoliation of graphite using serum from skim natural rubber latex in ultrasound-induced and shear-induced systems

Natchanon Jirasitthanit and Panu Danwanichakul\*

Department of Chemical Engineering, Faculty of Engineering, Thammasat School of Engineering, Thammasat University, Pathum Thani 12120, Thailand

Received 15 April 2023  
Revised 1 November 2023  
Accepted 10 November 2023

### Abstract

The green exfoliation of graphite using the serum from skim natural rubber latex, with some left-over ammonia, was investigated. The methods proposed to increase the exfoliation yield included varying the graphite concentration from 10 to 25 mg/ml of serum, using smaller graphite powders obtained from the sedimentation of a graphite precursor, and increasing rotor speed of a homogenizer. The two former cases were performed in an ultrasonic bath. In the first case, using 10 mg of graphite/ml of serum gave the maximum yield of 0.70%. In the second case of using graphite suspended in the supernatant after 15-min settling as starting material in exfoliation, the yield was increased to 0.74% at the graphite concentration of 25 mg/ml. In the last case, using the homogenizer probe at 5,400 rpm for 20 min gave the yield up to 10.5%. Based on Raman spectroscopy, all these exfoliated products were multilayer graphene-based materials and could be comparable to the commercial graphene-based product.

**Keywords:** Liquid-phase exfoliation, Ammonia, Skim natural rubber latex, Graphite, Graphene

### 1. Introduction

Graphene is one of the nanomaterials that could potentially be used in extensive applications including bendable touch screens, battery electrodes, and drug delivery materials [1] due to its high strength, light weight, great toughness, and excellent electrical and thermal properties at room temperature. It is a layer of  $sp^2$  carbon atoms bonded as connected hexagons in long sheet generating a two-dimensional (2D) system. Graphene-based materials are also of interest, including few-layer graphene (FLG) and multilayer graphene (MLG) which can be stacked layer by layer through van der Waals forces. The properties of MLG were different from those of FLG and single-layer graphene [2].

Like many nanomaterials, graphene could be produced from top-down and bottom-up processes. The former involves mechanical or chemical separation of graphite layers held together by weak van der Waals forces, while the latter involves arrangement of carbon atoms from a carbon source to form graphene via pyrolysis and chemical vapor deposition [1]. The most widely used top-down technique is a modified Hummers' method, in which graphite layers were oxidized in several steps with various strong oxidizing agents to make them more hydrophilic, thereby being easily exfoliated and dispersed in water as graphene oxide (GO). This technique produces a high yield but GO has a poorer electrical conductivity. Therefore, graphene oxide (GO) may be reduced to yield reduced graphene oxide (rGO). However, both GO and rGO may have strong acid-basic residues and large amounts of water were used in the processes [3-9]. Thus, exfoliation of graphite in the liquid phase by utilizing a variety of substances has been studied in conjunction with other techniques to minimize the use of hazardous chemicals and copious amounts of water while maintaining the electrical conductivity of products to the greatest extent possible.

In one technique, high shear was applied to separate graphite layers. For instance, high-shear mixing of graphite via a rotor-stator mixer was investigated. 10-ml suspension at the initial graphite concentration of 100 mg/ml was investigated with sodium cholate as a surfactant. The suspension was mixed at 16,500 rpm for 2 h. It was found that the graphene yield was 3% [10]. In addition, another work proposed scalable production of graphene by high-shear mixing of graphite via a rotor-stator mixer in N-methyl-2-pyrrolidone (NMP) or an aqueous surfactant solution of sodium cholate, but the separation yields were still relatively low (< 0.1%) [11]. Alternatively, the use of organic salts such as sodium citrate, potassium citrate (K-Citrate), and sodium tartrate together with NMP solution and a rotor-stator mixer at the speed of 9,000 rpm was proved to help separate the graphite surfaces. It was found that the exfoliation of 10 mg graphite in 1 ml NMP with K-Citrate produced a graphene yield of 10%, and up to 50% after 8 cycles of exfoliation [12].

Using an alternate technique, ultrasonication was utilized to separate graphite layers. For example, exfoliation using 5 g of graphite powder in 500 mL NMP (10 mg/ml) with ultrasonication (100 W, 40 kHz) for 48 h was studied. It was found that graphene was produced in a yield of 0.2%, and it was then used to construct an electrochemical sensor for the simultaneous determination of endocrine disruptors such as diethylstilbestrol and estradiol [13]. In other work, the direct exfoliation of graphite to produce few-layer graphene was investigated utilizing NMP in conjunction with ultrasonication at 240 – 600 W for 30 – 120 min. The maximum exfoliation yield

\*Corresponding author.

Email address: dpanu@engr.tu.ac.th

doi: 10.14456/easr.2024.5

of 19% was obtained at the initial concentration of 0.5 mg graphite/ml NMP. The yield rose to 20% when ultrasonication was applied for 90 minutes. The exfoliation efficiency was also improved in the presence of Fe<sub>3</sub>O<sub>4</sub> nanoparticles [14]. In addition, liquid exfoliation of graphite in polar solvents was investigated by utilizing ethanol and dimethylformamide (DMF) with ultrasonication (40 kHz, 130 W) at ultrasonication times of 2, 5, and 7 h and initial graphite concentrations of 0.5, 1, and 2 mg/ml. The DMF or ethanol solvent volume was maintained at 10 ml. After 7 h of ultrasonication, the exfoliation procedure gave a maximum yield of 2.2% in ethanol and 9.6% in DMF [15].

Water has been the most interesting liquid in the exfoliation of graphite because it is cheap and harmless. It has been reported that to generate a suspension of a monolayer or multilayer graphene, alkaline aqueous solutions or water containing various organic surfactants may be used, together with ultrasonication at high and low frequencies (1174 kHz and 20 kHz) generating a 10% graphene yield [16]. In another work, urea was used in the exfoliation of graphite in pure water, producing a high-quality graphene sheet. 1 g of graphite was dispersed in 100 mL of urea solution (100 ml DI water and 100 g urea), and it was then ultrasonicated for 2 h at room temperature. The result showed a yield of 0.12% [17]. In addition, it was found that ammonia could play an important role in graphite exfoliation in purified water. 4000 mg of graphite powder was added to an ammonia solution to achieve a concentration of 20 mg/ml. The mixture of graphite and water was ultrasonicated for 2 h, resulting in high-quality graphene sheets with a graphene yield of 0.29% [18].

Based on the idea of using ammonia solution for the exfoliation of graphite [18], it is of great interest to utilize the serum from the skim natural rubber latex (SNRL), with high-content ammonia residue, for this application. SNRL is a by-product from the concentrated latex production - one of the major agricultural products of Thailand. For instance, 964,403 tons of concentrated latex were produced, yielding 1,155,355 tons of SNRL in 2015 [19]. SNRL contains 4 – 7% rubber particles (cis-1,4-polyisoprene) and many organic substances including sugars, fatty acids, proteins, and ammonia in a large amount of water [20]. SNRL is, therefore, potentially used as a dispersing agent in graphite exfoliation.

Ammonia is added in two steps in the production of concentrated latex. First, it is added to the field natural rubber latex (FNRL) to prevent bacterial attack and increase colloidal stability. Second, it is added to boost stability during centrifugation to yield concentrated latex and SNRL. In general, rubber particles in SNRL are coagulated with sulfuric acid (H<sub>2</sub>SO<sub>4</sub>) generating highly acidic serum as wastewater to be treated, which is unfriendly to the environment. Research work investigated new coagulation media for rubber coagulation, including chitosan in acetic acid solution and aqueous cationic polyacrylamide (PAM+) solution [21]. Upon utilizing PAM+, the serums which contained organic materials such as fatty acids, carbohydrates, and proteins, as well as the ammonia, were used as reducing and stabilizing agents in the creation of metallic nanoparticles including silver and gold nanoparticles [22-25]. In this work, only ammonia was investigated as an effective dispersing agent in the exfoliation of graphite. In our preliminary work, the exfoliation yield when using graphite concentration at 25 mg/ml serum together with ultrasonication was 0.28 – 0.43% [26] and this is used as a reference for comparison. In the current work, the exfoliation yield was expected to be increased with three proposed methods: (1) varying the concentration of graphite in the serum in the ultrasonic system; (2) separating smaller graphite powders from the precursor graphite and using them as starting materials in the ultrasonic system; and (3) using a homogenizer (rotor-stator mixer) instead of an ultrasonic bath.

## 2. Materials and methods

### 2.1 Materials

Graphite powder (particle size less than 50 µm) was purchased from Merck & Co., Inc. Skim natural rubber latex (SNRL) and cationic polyacrylamide (PAM+) were supplied by Thai Eastern Group Holdings Public Co., Ltd. (Thailand) and Welkin Enterprise Co., Ltd. (Thailand), respectively. Sodium dodecyl sulfate (SDS) was purchased from Ajax Finechem. The commercial multilayer graphene-based product was provided by TCI Co., Ltd. (thickness 6 – 8 nm, width 5 µm).

### 2.2 Preparation of the serum from SNRL

200 ml of 0.7% wt/vol PAM+ solution was prepared as the coagulation medium and added to 250 ml of SNRL, and the mixture was stirred at a low speed of 200 rpm to coagulate the rubber particles in the SNRL. After that, the coagulum was removed and filtered with a piece of nylon fabric and the clear yellowish liquid called the serum was obtained. The pH value of the serum was measured with a pH meter.

### 2.3 Liquid phase exfoliation of graphite

The schemes of three paths to increase the exfoliation yield are shown in Figure 1. In the first path, varying the graphite concentration in the serum was investigated, as detailed in section 2.3.1. The second path involved the separation of smaller graphite powders first and using those as starting materials for exfoliation, as explained in section 2.3.2. Finally, the third path applied a homogenizer instead of an ultrasonic bath in the exfoliation process, as discussed in section 2.3.3.

#### 2.3.1 Ultrasonication-assisted exfoliation of graphite using various graphite concentrations

The graphite concentrations of 10 – 25 mg/ml were prepared by mixing 100 – 250 mg of graphite powder with 10 ml of serum from SNRL with a pH of 9.33. The mixture was sonicated for 2 h in an ultrasonic bath (200 W, 40 kHz). The starting temperature was 29°C and increased to 53°C in 15 min and was at 53°C throughout the experiment. Next, the solution was left standing for 2 h for sedimentation at room temperature. The supernatant of the mixture was sampled and centrifuged at 2,000 rpm (equivalent to RCF of 224) for 30 min and separated into upper and lower sections. The upper one was then centrifuged at 10,500 rpm (equivalent to RCF of 6,163) for 30 min to collect the samples in 1.5 ml micro-centrifuge tubes. Each collected sample was washed with 1% wt/vol sodium dodecyl sulfate (SDS) solution and thereafter with distilled water, and dried in an oven at 80°C until its weight was constant. The samples were called G-100 to G-250 and were chosen for characterization, as discussed in section 3.4. The percentage yield of each sample can be calculated from:

$$\% \text{ yield} = \frac{\text{weight of the exfoliated graphite sample}(g)}{\text{weight of the precursor graphite}(g)} \times 100 \quad (1)$$

### 2.3.2 Ultrasonication-assisted exfoliation of smaller graphite powders

The precursor graphite powders were separated according to their weights by sedimentation at room temperature. Initially, 500 mg of graphite was dispersed in 30 ml of distilled water using a vortex mixer. After that, it was left standing for 15, 30, or 45 seconds. The heavier graphite powders settled down and the top section of liquid was transferred to a beaker and dried at 80°C. The solid powders then underwent the exfoliation process presented in section 2.3.1 by using 250 mg of graphite and 10 ml of the serum at a pH of 9.33. The samples were called G-15s, G-30s, and G45s and they were characterized in section 2.4. The percentage yield of each sample can be calculated using Eq. (1).



**Figure 1** The schemes of graphite exfoliation in three proposed paths to yield various exfoliated graphite samples are proposed.

### 2.3.3 Shear-assisted exfoliation of graphite with a homogenizer probe

The graphite concentration of 25 mg/ml was prepared by mixing 250 mg of graphite powder with 10 ml of serum from SNRL with a pH between 8.91 – 9.12. The mixture was treated with a homogenizer probe (rotor D = 12.5 mm and stator D = 18 mm) at 5,400 rpm for 20 min, 5,400 rpm for 30 min, and 8,100 rpm for 20 min. The mixture was centrifuged at 1,000 rpm for 3 min to remove bubbles, and then left for 2 h for sedimentation. The supernatant was put in tubes and centrifuged at 10,500 rpm for 30 min to collect the samples. Each collected sample was washed, and dried in an oven at 80°C until the weight was constant. The samples were called G-5400/20, G-5400/30, and G-8000/20 and they were characterized as discussed in section 2.4. The percentage yield of each sample was obtained using Eq. (1).

The yields of exfoliated graphite samples from the experiments following Path #1, Path #2, and Path #3 are reported in Table 1 as the average yields obtained from three replicates.

**Table 1** Percentage yields of the exfoliated graphite samples from three proposed methods are reported.

Method	Starting material for exfoliation	Condition	mg graphite/ 10 ml of serum	Sample	% Yield
Path #1: Ultrasonication	As-received graphite	-Varying initial graphite concentration -Ultrasonication for 2 h at 53°C	100	G-100	0.70 ± 0.10
			125	G-125	0.56 ± 0.12
			150	G-150	0.62 ± 0.14
			175	G-175	0.44 ± 0.09
			200	G-200	0.27 ± 0.08
			225	G-225	0.34 ± 0.07
Path #2: Separation and Ultrasonication	Smaller graphite powders were prepared at different settling time of 15, 30 and 45 s and used as starting materials	-Smaller graphite powders -Ultrasonication for 2 h at 53°C	250	G-15s	0.74 ± 0.44
			250	G-30s	1.06 ± 0.61
			250	G-45s	1.56 ± 0.95
Path #3: Homogenizer Probe	As-received graphite	-Homogenizer probe applied at different speed (5,400 and 8,100 rpm) and time (20 and 30 min)	250	G-5400/20	10.05 ± 1.46
			250	G-5400/30	10.90 ± 2.71
			250	G-8100/20	13.23 ± 1.75

## 2.4 Characterization of the exfoliated graphite

### 2.4.1 Raman Spectroscopy

Raman spectroscopy results of the chosen exfoliated graphite samples (G-100, G-250, G-15s, G-30s, G-45s, G-5400/20, G-5400/30, G-8100/20) were obtained using a dispersive Raman microscope (Bruker Optics, Model: Senterra) with the laser wavelength at 532 nm, the laser power of 5 mW and the spectral range of 4500 – 700  $\text{cm}^{-1}$ . The measurement followed the standard methods, ASTM: E1693 and ASTM: E1840.

### 2.4.2 Scanning electron microscopy (SEM)

The structures and surface morphology of the chosen exfoliated graphite samples were investigated using a scanning electron microscope (SEM, JSM-7800F) with an accelerating voltage of 15 kV. The magnification was adjusted to 10,000 $\times$ .

## 3. Results and discussion

### 3.1 The yield of exfoliated graphite samples from different liquid exfoliation processes

As can be seen in Table 1, the yields of using ultrasonic bath method were lower than those of the homogenizer probe. Upon decreasing the graphite concentration in the ultrasonic bath, the yield was first decreased from 0.43% (G-250) to 0.27% (G-200) and then increased to 0.70% (G-100). These yields were much less than the reported values of 19% and 20% when using NMP solvents together with sonication [13, 14]. But the yield of G-200, the same graphite concentration used in the system of ammonia solution at pH 9 in the literature [18], was about the same as the reported value of 0.29%, confirming the effect of residual ammonia in the serum of SNRL.

It was evident that after the removal of heavier graphite powders using the sedimentation process, the smaller graphite powders gave higher exfoliation yields. The settling time was varied 15, 30, and 45 s in order to obtain the supernatant with smaller suspended powders. The weight of graphite powder is related to either its lateral dimension or its thickness, or both.

The method to impart energy to graphite powder was changed to shear mode in Path#3. It was found that the use of a homogenizer helped delaminate more graphite powders, which was consistent with some research on high-shear mixing of graphite via a rotor-stator mixer at a speed of 9,000 rpm. The exfoliation of 10 mg graphite in 1 ml of NMP with K-Citrate yielded a graphene yield of 10% [12]. It was found that our results were slightly higher than those reported. Upon increasing the rotor speed of the homogenizer probe, exfoliation yield could be increased due to the increase in shear stress. The exfoliation time from 20 to 30 min could also slightly increase the yield.

### 3.2 Characterization of the exfoliated graphite

#### 3.2.1 Raman spectroscopy results

Raman scattering was used to assess the characteristics of the exfoliated graphite samples, precursor graphite, and commercial graphene-based product, since it is particularly sensitive to crystal flaws and the number of layers in graphite and graphene sheets. In the measurement, the laser photons excite the electron-hole pairs leading to the inelastic scattering of the electrons and holes by phonon emission/absorption and elastic scattering of the electrons mediated by the defect and recombination of the electron-hole pair. The usual three primary peaks are D-peak at  $\sim 1350 \text{ cm}^{-1}$ , G-peak at  $\sim 1580 \text{ cm}^{-1}$ , and 2D-peak at  $\sim 2700 \text{ cm}^{-1}$ . A secondary peak such as D'-peak at  $1620 \text{ cm}^{-1}$  was also reported [16, 27]. Raman spectroscopy results of the chosen exfoliated samples are shown in Figure 2 and Table 2. Figure 2 (a) showed the Raman spectroscopy result of the sample G-250 before washing, where all the peaks were mostly obscured by the impurity. The peaks appeared clearly in Figure 2(b) after the sample was washed twice with SDS solution and water.

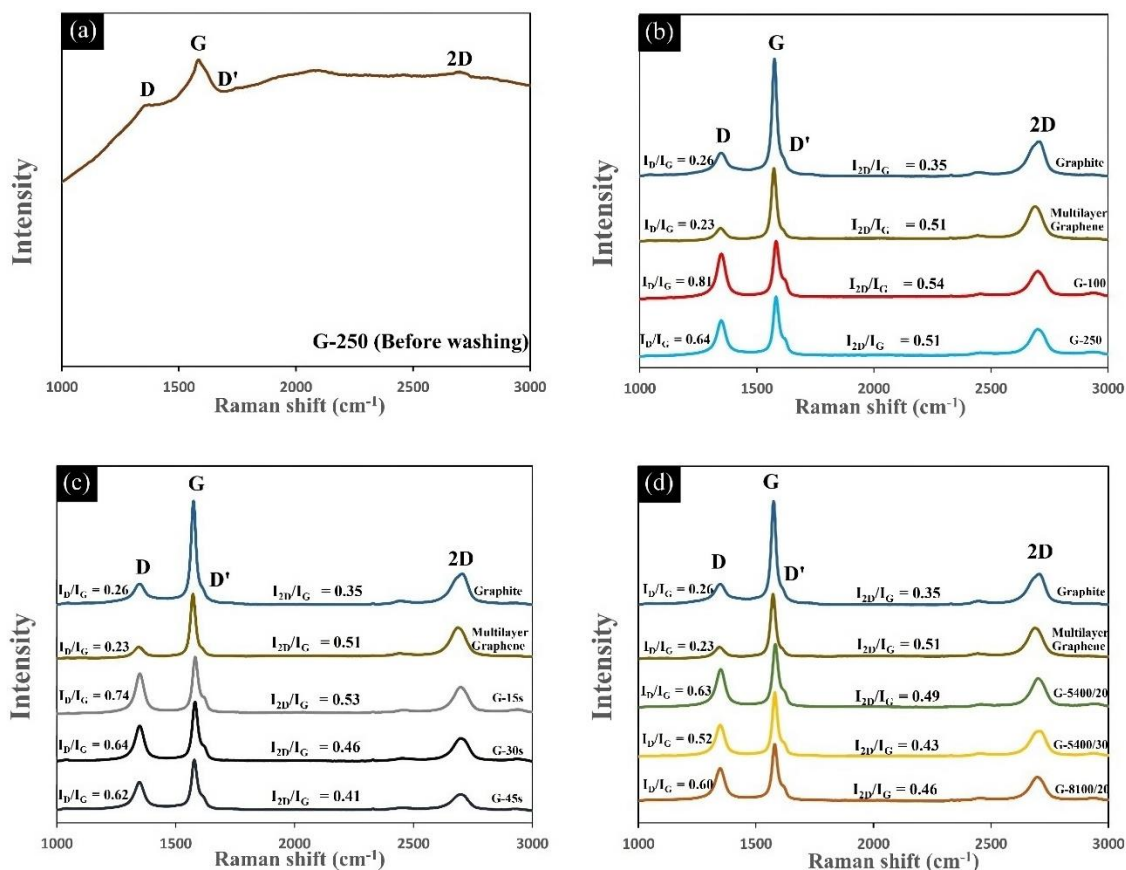


**Figure 2** Raman spectra of the exfoliated samples are compared with the precursor graphite and the commercial multilayer graphene-based product: (a) G-250 before washing with SDS solution and water, (b) G-100 and G-250 from Path #1, (c) G-15s, G-30s and G-45s from Path #2, and (d) G-5400/20, G-5400/30 and G-8100/20 from Path #3.

D-peak occurs due to the elastic scattering of the electron by one phonon before being mediated by the defect, so it indicates the presence of defects in graphitic materials. Thus, there is no D-peak for a perfect single-layer graphene. Defects include: (1) the disorder at the edges of all layers which might be from nanoscale roughness; (2) vacancies in the structures; and (3)  $sp^3$ -type defect from the functionalization of carbon atoms. In addition, a secondary peak, D'-peak, which is adjacent to G-peak also indicates the presence of defects. The ratio of  $I_D/I_{D'}$  signifies the type of defect. According to the literature [2], the value of the ratio could reach about 13 for  $sp^3$ -type defect, about 7 for vacancies, and about 3.5 for boundaries. The values of this ratio for our samples were 1.71 – 2.17, implying that the defects were primarily from the edge disorders.

**Table 2** Results from Raman spectra, including primary peak positions, intensities, and the corresponding ratios of peak intensities of the exfoliated samples are shown.

Sample	D-peak (cm <sup>-1</sup> )	I <sub>D</sub>	G-peak (cm <sup>-1</sup> )	I <sub>G</sub>	2D-peak (cm <sup>-1</sup> )	I <sub>2D</sub>	2D-FWHM (cm <sup>-1</sup> )	I <sub>D</sub> /I <sub>G</sub>	I <sub>2D</sub> /I <sub>G</sub>
G-100	1348.0	5271.9	1582.5	6526.8	2700.0	3553.2	72.9	0.81	0.55
G-250	1348.0	4129.8	1582.0	6521.6	2699.5	3293.9	73.5	0.64	0.50
G-5400/20	1350.5	4729.8	1582.0	7541.1	2700.5	3705.1	69.9	0.63	0.49
G-5400/30	1348.0	3950.5	1580.5	7617.5	2708.0	3290.2	76.3	0.52	0.43
G-8100/20	1348.0	4115.4	1579.5	6823.2	2696.5	3125.8	72.0	0.60	0.45
G-15s	1348.5	5213.6	1582.5	7081.6	2699.0	3722.6	70.4	0.74	0.53
G-30s	1348.5	4863.2	1581.5	7542.2	2699.5	3466.8	74.7	0.64	0.46
G-45s	1347.0	4036.4	1578.5	6546.7	2694.5	2654.3	77.5	0.62	0.41
Graphite	1347.8	3265.2	1575.1	12580.1	2706.0	4404.7	79.1	0.26	0.35
Multilayer graphene-based product	1344.2	1817.0	1572.9	7739.2	2686.2	3967.6	74.4	0.23	0.46

G-peak represents C–C in-plane vibrational in  $sp^2$  hybridized carbon bonds in the graphene or graphite lattice [15]. It is sensitive to external perturbations such as defects, doping, strain and temperature [2]. In theory, a plane with larger spatial dimension could yield a higher degree of C–C stretching and more edge defects. Therefore, it is common to compare  $I_D/I_G$  ratios of the samples in order to attenuate the effect of spatial dimension when studying the edge defects [28–30]. For graphene with very few layers, it was reported that the value of  $I_D/I_G$  increased with defect density in the low defect density region to a maximum of 3.5 and then decreased in the high defect density region [31]. In our case, there were no chemical reactions involved and the values of  $I_D/I_G$  were much less than 3.5, so it should be in the low defect density region where the values of the ratio increased with the defect density.

Table 2 shows that upon decreasing the concentration of graphite used (from 25 to 10 mg/ml), the value of  $I_D/I_G$  increased, implying more disordered edges were exposed. When using smaller graphite powders, the value decreased unexpectedly with the powder size (i.e., shorter settling time), implying that exfoliation might be better for larger powders.

It was also found that applying sonication with heating could yield samples with higher values of  $I_D/I_G$  than using the homogenizer probe, possibly because more edge defects may be caused by ultrasonication with heating. In contrast to the reduced graphene oxide sheets produced by using the chemical oxidation-reduction method, whose  $I_D/I_G$  ratio was between 1.1 – 1.5 [27], those of our samples were still much lower. The value of  $I_D/I_G$  of all samples were greater than that of precursor graphite and the commercial graphene-based product, indicating that the edge defects were generated during exfoliations in all methods.

Furthermore, 2D-peak is related to the number of graphene layers [29, 30]. Generally,  $I_{2D}/I_G$  decreased as the number of layers increased but it is not enough to determine the number of layers due to interference from doping and laser polarization effect [32]. For multilayer graphene whose edge defects increased with the number of layers, 2D-peak appears due to the scattering of an electron by two phonons before it recombines with the hole; if electrons are mediated with the defects, fewer numbers of electrons will be recombined with the holes, resulting in a lower intensity 2D-peak [2, 32]. It was stated that this ratio could be increased by exfoliation from 0.35 to 0.50 for multilayer graphene to 0.69 for bilayer graphene [27].

In Table 2, the values of  $I_{2D}/I_G$  of all samples were greater than that of graphite (0.35) and comparable to or greater than that of commercial graphene-based product (0.50), indicating that the precursor graphite was truly exfoliated in every method. It was also seen that when lowering the amount of graphite to ml of serum from 25 to 10 mg/ml, graphite could be more exfoliated. Similarly, the  $I_{2D}/I_G$  showed the same trend as the  $I_D/I_G$  when using smaller graphite powders as discussed earlier. This confirms that exfoliation of heavier graphite was more effective. It is consistent with work focusing on using ultrasonication to reduce the size of biomass in the treatment of municipal wastewater. It was reported that suspended solids with larger sizes were prone to higher degree of breakage, especially at higher ultrasound energy density [33]. Regarding the homogenizer method, it can be seen that applying 5,400 rpm for 20 min was more effective than 8,000 rpm for 20 min, which in turn was more effective than 5,400 rpm for 30 min.

Interestingly another parameter, the full width at half maximum (FWHM) of 2D-peak exhibited the opposite trend against  $I_{2D}/I_G$  in each group of the experiments. The FWHM is used to relate to the number of layers of graphitic materials too. The FWHM of 2D-peak is wider for the sample with a higher number of layers because 2D-peak is, in fact, comprised of constructive interferences of all peaks generated by each layer [31]. Obviously, all samples had narrower FWHM than the precursor graphite. The FWHM of 2D-peak was reported for single-layer, bilayer, trilayer, four-layer and five-layer graphene [32]. The FWHM of five-layer graphene was between 65 and 67.5  $cm^{-1}$ . Therefore, all the obtained samples should be composed of more than 5 layers.

### 3.2.2 SEM micrographs

The morphology of the dried exfoliated graphite samples in the previous section was observed through SEM micrographs in Figure 3. The micrographs showed stacks of many apparent sheets, in fact each apparent sheet is composed of many atomic layers of graphene packed together, which could not be observed via SEM at the magnification of 10,000. According to the scale bar on the SEM micrograph, each figure covers the area of  $10 \times 12 \mu m^2$ . Figures 3 (a) – 3 (b) showed samples from different initial concentrations of graphite. Figures 3 (f) – 3 (h) showed samples undergoing ultrasonication when being exfoliated, but the separation of graphite sizes was done prior to the exfoliation process. The structures looked quite similar in Figures 3 (a) – 3 (b) and 3 (f) – 3 (h). The cracked exfoliated graphite sheets with visible edges may be caused by sonication with heating. In Figures 3 (c) – 3 (e), the samples obtained from using the homogenizer probe were shown. The larger plates with clear edges were seen with some fragments around, possibly caused by the shear stress which was dependent on the rotor speed of the homogenizer probe.

## 4. Conclusions

This work proposed three paths to increase the exfoliation yield of graphite powders when using the serum from skim natural rubber latex with the left-over ammonia as the dispersing agent. The first two paths involved varying the concentration of graphite and using smaller graphite powders, both in the ultrasonic system. In the last path, the homogenizer probe was used instead of the ultrasonic bath. All three paths could increase the exfoliation yields of exfoliated graphite, especially the last one, in which the yield could be boosted up to 30 times the yield of the reference sample in our preliminary work (0.4%), where the concentration of 25-mg graphite/ml serum was used in the ultrasonic system.

According to Raman spectroscopy results, multilayer graphene-based products were obtained for all cases because 2D-peaks were not sharp with FWHM between 69.9 and 77.5  $cm^{-1}$ . It was found that the sample using the graphite concentration in the serum at 10 mg/ml (G-100) gave the exfoliated graphite with fewer layers and higher yields than the reference case of 25 mg/ml in the ultrasonic bath. Using smaller graphite powders could also yield fewer layers if the size of the powder was not too small (FWHM of G-15s was greater than G-30s and G-45s). The SEM micrographs showed the stacks of apparent sheets with various lateral sizes in microscale and could not be differentiated much from one another.

It is of great interest to investigate the dispersing ability of the exfoliated products in pure water, or any solvent of interest, as well as the adsorption capacity of the products for practical use as adsorbents or drug carriers. The experiments should be done in comparison with the precursor graphite and the commercial multilayer graphene-based product.



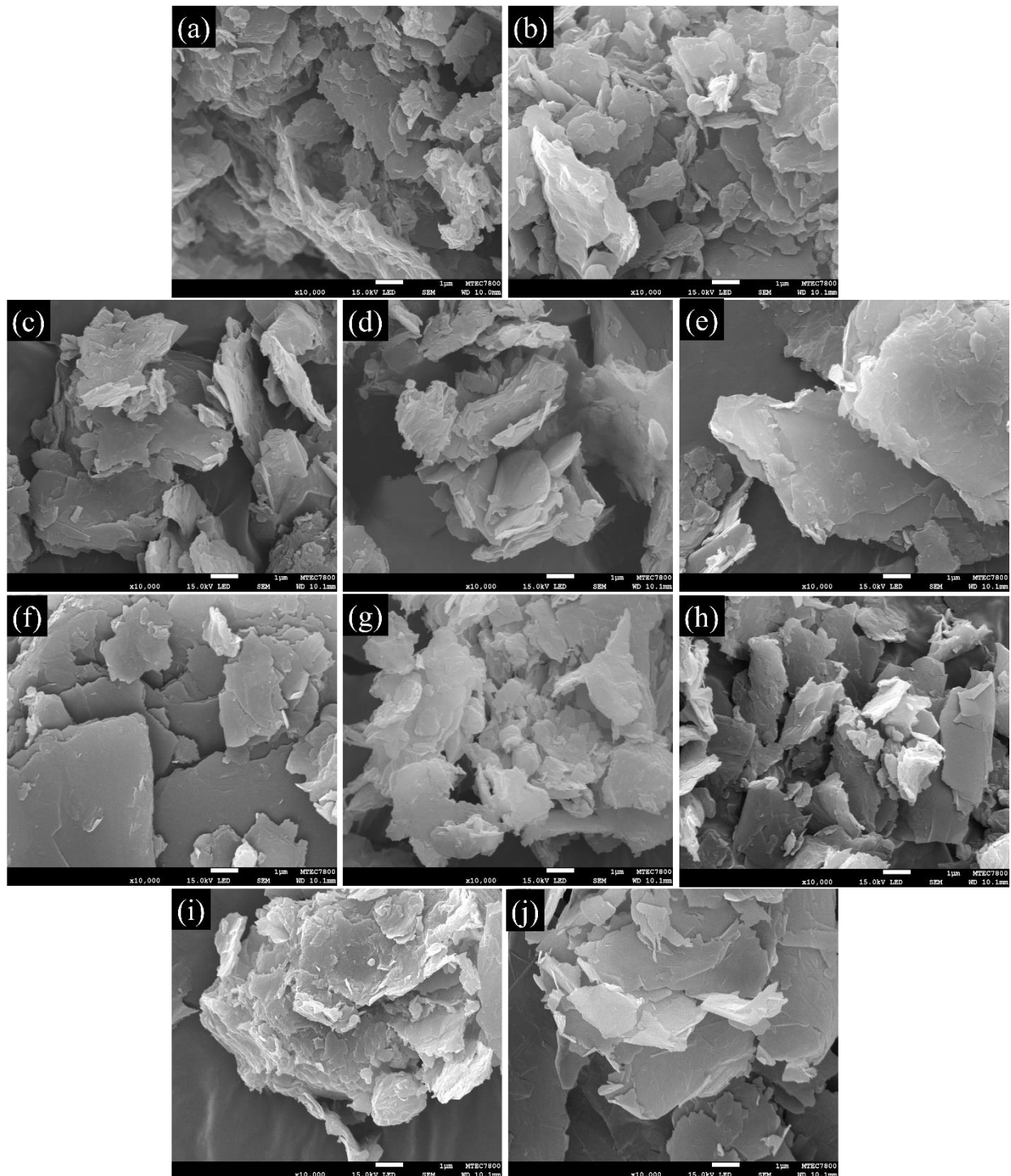


**Figure 3** SEM images of the exfoliated graphite samples are shown: (a) G-100, (b) G-250, from the experiments of varying initial graphite concentration (Path #1), (c) G-5400/20, (d) G-5400/30, (e) G-8100/20, from those using homogenizer probe (Path #3), (f) G-15s, (g) G-30s, (h) G-45s, from those using smaller graphite powders (Path #2), (i) the precursor graphite and (j) the commercial graphene-based product.

## 5. Acknowledgements

The authors would like to acknowledge the Department of Chemical Engineering and the Faculty of Engineering, Thammasat School of Engineering, Thammasat University for the financial support of this work. Natchanon Jirasitthanit is also grateful to the Thammasat School of Engineering, Faculty of Engineering for the Graduate Scholarship.

## 6. References

- [1] Srikaew M, Saengsuwan S. Graphene (The Miracle Material): strategies for synthesis, properties, development, characterizations and applications. *J Sci Tech UBU*. 2020;22(2):39-49. (In Thai)

- [2] Wu JB, Lin ML, Cong X, Liu HN, Tan PH. Raman spectroscopy of graphene-based materials and its applications in related devices. *Chem Soc Rev*. 2018;47(5):1822-73.
- [3] Hummers Jr. WS, Offeman RE. Preparation of graphitic oxide. *J Am Chem Soc*. 1958;80(6):1339.
- [4] Edwards RS, Coleman KS. Graphene synthesis: relationship to applications. *Nanoscale*. 2013;5(1):38-51.
- [5] Kusriani E, Ramadhani I, Alhamid MI, Voo NY, Usman A. Synthesis and adsorption performance of graphene oxide-polyurethane sponge for oil-water separation. *Eng J*. 2022;26(1):1-9.
- [6] Thema FT, Moloto MJ, Dikio ED, Nyangiwe NN, Kotsedi L, Maaza M, et al. Synthesis and characterization of graphene thin films by chemical reduction of exfoliated and intercalated graphite oxide. *J Chem*. 2013;2013:150536.
- [7] Rasoulzadehzali M, Namazi H. Facile preparation of antibacterial chitosan/graphene oxide-Ag bio-nanocomposite hydrogel beads for controlled release of doxorubicin. *Int J Biol Macromol*. 2018;116:54-63.
- [8] Zaaba NI, Foo KL, Hashim U, Tan SJ, Liu WW, Voon CH. Synthesis of graphene oxide using modified hummers method: solvent influence. *Procedia Eng*. 2017;184:469-77.
- [9] Nazri SRB, Liu WW, Khe CS, Hidayah NMS, Teoh YP, Voon CH, et al. Synthesis, characterization and study of graphene oxide. *AIP Conf Proc*. 2018;2045(2):020033.
- [10] Lund S, Kauppila J, Sirkiä S, Palosaari J, Eklund O, Latonen RM, et al. Fast high-shear exfoliation of natural flake graphite with temperature control and high yield. *Carbon*. 2021;174:123-31.
- [11] Paton KR, Varrla E, Backes C, Smith RJ, Khan U, O'Neill A, et al. Scalable production of large quantities of defect-free few-layer graphene by shear exfoliation in liquids. *Nat Mater*. 2014;13(6):624-30.
- [12] Liang B, Liu K, Liu P, Qian L, Zhao G, Pan W, et al. Organic salt-assisted liquid-phase shear exfoliation of expanded graphite into graphene nanosheets. *J Mater*. 2021;7(6):1181-9.
- [13] Hu L, Cheng Q, Chen D, Ma M, Wu K. Liquid-phase exfoliated graphene as highly-sensitive sensor for simultaneous determination of endocrine disruptors: diethylstilbestrol and estradiol. *J Hazard Mater*. 2015;283:157-63.
- [14] Hadi A, Zahirifar J, Karimi-Sabet J, Dastbaz A. Graphene nanosheets preparation using magnetic nanoparticle assisted liquid phase exfoliation of graphite: the coupled effect of ultrasound and wedging nanoparticles. *Ultrason Sonochem*. 2018;44:204-14.
- [15] Gomez CV, Guevara M, Tene T, Villamagua L, Usca GT, Maldonado F, et al. The liquid exfoliation of graphene in polar solvents. *Appl Surf Sci*. 2021;546:149046.
- [16] Tyurnina AV, Morton JA, Subroto T, Khavari M, Maciejewska B, Mi J, et al. Environment friendly dual-frequency ultrasonic exfoliation of few-layer graphene. *Carbon*. 2021;185:536-45.
- [17] Hou D, Liu Q, Wang X, Qiao Z, Wu Y, Xu B, et al. Urea-assisted liquid-phase exfoliation of natural graphite into few-layer graphene. *Chem Phys Lett*. 2018;700:108-13.
- [18] Ma H, Shen Z, Yi M, Ben S, Liang S, Liu L, et al. Direct exfoliation of graphite in water with addition of ammonia solution. *J Colloid Interface Sci*. 2017;503:68-75.
- [19] Khetsofopon V. Look at the direction of Thai rubber in year 62, rising or falling?. Hat Yai, Songkhla; Thai Latex Association; 2019.
- [20] Danwanichakul P, Suwatthanarak T, Suwanvisith C, Danwanichakul D. The role of ammonia in synthesis of silver nanoparticles in skim natural rubber latex. *J Nanosci*. 2016;2016:7258313.
- [21] Danwanichakul P, Werathirachot R, Kongkaew C, Loykulnant S. Coagulation of skim natural rubber latex using chitosan or polyacrylamide as an alternative to sulfuric acid. *Eur J Sci Res*. 2011;62(4):537-47.
- [22] Suwatthanarak T, Than-ardna B, Danwanichakul D, Danwanichakul P. Synthesis of silver nanoparticles in skim natural rubber latex at room temperature. *Mater Lett*. 2016;168:31-5.
- [23] Jullabuth T, Danwanichakul P. Silver nanoparticle synthesis using the serum obtained after rubber coagulation of skim natural rubber latex with chitosan solution. *Eng Appl Sci Res*. 2021;48(4):422-31.
- [24] Pongsanon P, Danwanichakul D. Synthesis of gold nanoparticles using serum from skim natural rubber latex: the effect of remaining coagulants. *TSTJ*. 2020;28(4):596-606. (In Thai)
- [25] Chetia L, Kalita D, Ahmed GA. Synthesis of Ag nanoparticles using diatom cells for ammonia sensing. *Sens Biosensing Res*. 2017;16:55-61.
- [26] Nabnean W, Jirasitthanit N. Exfoliation of graphite using natural substances [thesis]. Pathum Thani: Thammasat University; 2020.
- [27] Navik R, Gai Y, Wang W, Zhao Y. Curcumin-assisted ultrasound exfoliation of graphite to graphene in ethanol. *Ultrason Sonochem*. 2018;48:96-102.
- [28] Ma F, Liu L, Wang X, Jing M, Tan W, Hao X. Rapid production of few layer graphene for energy storage via dry exfoliation of expansible graphite. *Compos Sci Technol*. 2020;185:107895.
- [29] Liu X, Liu J, Zhan D, Yan J, Wang J, Chao D, et al. Repeated microwave-assisted exfoliation of expandable graphite for the preparation of large scale and high quality multi-layer graphene. *RSC Adv*. 2013;3(29):11601-6.
- [30] Savi P, Yasir M, Giorcelli M, Tagliaferro A. The effect of carbon nanotubes concentration on complex permittivity of nanocomposites. *Prog Electromagn Res M*. 2017;55:203-9.
- [31] Childres I, Jauregui LA, Park W, Cao H, Chen YP. Raman spectroscopy of graphene and related materials. In: Jang JI, editor. *New developments in photon and materials research*. New York: Nova Science Publishers; 2013. p. 1-20.
- [32] Li Z, Deng L, Kinloch IA, Young RJ. Raman spectroscopy of carbon materials and their composites: graphene, nanotubes and fibres. *Prog Mater Sci*. 2023;135:101089.
- [33] Gibson JH, Hon H, Farnood R, Droppo IG, Seto P. Effects of ultrasound on suspended particles in municipal wastewater. *Water Res*. 2009;43(8):2251-9.